Tensor-polarized structure function b_1 in the standard convolution description of the deuteron

W. Cosyn,[1] Yu-Bing Dong,[2,3] S. Kumano,[4,5] and M. Sargsian[6]

[1]*Department of Physics and Astronomy, Ghent University, Proeftuinstraat 86, B9000 Ghent, Belgium*
[2]*Institute of High Energy Physics, Chinese Academy of Sciences, Beijing 100049, China*
[3]*Theoretical Physics Center for Science Facilities (TPCSF), CAS, Beijing 100049, China*
[4]*KEK Theory Center, Institute of Particle and Nuclear Studies, High Energy Accelerator Research Organization (KEK), 1-1, Ooho, Tsukuba, Ibaraki 305-0801, Japan*
[5]*J-PARC Branch, KEK Theory Center, Institute of Particle and Nuclear Studies, KEK, and Theory Group, Particle and Nuclear Physics Division, J-PARC Center, 203-1, Shirakata, Tokai, Ibaraki 319-1106, Japan*
[6]*Department of Physics, Florida International University, Miami, Florida 33199, USA*

Tensor-polarized structure functions of a spin-1 hadron are additional observables, which do not exist for the spin-1/2 nucleon. They could probe novel aspects of the internal hadron structure. Twist-2 tensor-polarized structure functions are b_1 and b_2, and they are related by the Callan-Gross-like relation in the Bjorken scaling limit. In this work, we theoretically calculate b_1 in the standard convolution description for the deuteron. Two different theoretical models, a basic convolution description and a virtual nucleon approximation, are used for calculating b_1, and their results are compared with the HERMES measurement. We found large differences between our theoretical results and the data. Although there is still room to improve by considering higher-twist effects and in the experimental extraction of b_1 from the spin asymmetry A_{zz}, there is a possibility that the large differences require physics beyond the standard deuteron model for their interpretation. Future b_1 studies could shed light on a new field of hadron physics. In particular, detailed experimental studies of b_1 will start soon at the Thomas Jefferson National Accelerator Facility. In addition, there are possibilities to investigate tensor-polarized parton distribution functions and b_1 at Fermi National Accelerator Laboratory and a future electron-ion collider. Therefore, further theoretical studies are needed for understanding the tensor structure of the spin-1 deuteron, including a new mechanism to explain the large differences between the current data and our theoretical results.

I. INTRODUCTION

Spin structure of the nucleon has been investigated extensively, especially after the European Muon Collaboration discovery on the small quark-spin contribution to the nucleon spin. Now, its studies are focused on gluon-spin and orbital-angular-momentum effects. On the other hand, a spin-1 hadron has a richer spin structure than the spin-1/2 nucleon in the sense that there are four additional structure functions in the charged-lepton inclusive deep inelastic scattering (DIS) [1,2]. They are named b_1, b_2, b_3, and b_4 [2], which are associated with the tensor structure of the spin-1 hadron. The leading-twist structure functions are b_1 and b_2, and they are related to each other by the Callan-Gross-like relation $2x_D b_1 = b_2$, where x_D is the scaling variable for the spin-1 hadron, in the Bjorken scaling limit. These additional structure functions are interesting quantities for probing different dynamical aspects of the hadron structure, possibly of an exotic nature as we suggest in this article, from the ones for the spin-1/2 nucleon.

Within the parton model, the structure function b_1 satisfies the sum $\int dx b_1(x) = 0$ [3], where x is the Bjorken scaling

variable, by considering only the valence-quark part for the tensor structure. However, it does not mean $b_1(x) = 0$ for actual hadrons. In the fixed-target DIS, the simplest stable spin-1 target is the deuteron. If the deuteron b_1 is calculated in the convolution model [2,4], it is, in fact, finite and shows an oscillatory behavior as a function of x. Furthermore, shadowing mechanisms contribute significantly to b_1 at small x [5,6], and pions in the deuteron could also play a role [7]. There are related studies to the spin-1 hadron structure on a polarized proton-deuteron Drell-Yan process [8–10], leptoproduction of a spin-one hadron [11], fragmentation functions [12], generalized parton distributions [13], target-mass corrections [14], positivity constraints [15], lattice QCD estimates [16], and angular momenta for the spin-1 hadron [17]. The spin-1 deuteron structure can be also investigated by tagging the final state proton [18]. In addition, it is a unique opportunity to investigate the gluon transversity distribution, which exists only for hadrons with spin ≥ 1 [19].

The first measurement of b_1 was reported by the HERMES Collaboration in 2005 [20], and possible tensor-polarized parton distribution functions (PDFs) were extracted from the data [21]. The HERMES data are much

larger in magnitude compared to the conventional convolution calculation of Refs. [2,4]. It indicates that a new hadron mechanism should possibly be considered to interpret the large magnitude of b_1. As such an exotic mechanism, a contribution from a hidden-color state is proposed as a possibility together with a pionic contribution in Ref. [7].

The deuteron tensor structure has been investigated for a long time at low energies in terms of hadron degrees of freedom, and it originates from the D-state admixture in a bound proton-neutron system. However, time has come to investigate the tensor structure in terms of quark and gluon degrees of freedom through the structure functions b_{1-4}. In particular, the HERMES data seem to suggest a possible existence of an exotic hadron mechanism for interpreting their data because they deviate significantly from a conventional theoretical prediction. For describing nuclear structure functions at medium and large x, it is standard to use a convolution formalism, where a nuclear structure function is given by the corresponding one convoluted with a nucleon momentum distribution in a nucleus [22–24]. It is considered as a baseline calculation in describing nuclear modifications of F_2 at medium and large x in terms of the nuclear binding, Fermi motion, and short-range correlations embedded in the spectral function of the nucleon. We can use the same model for the deuteron in describing the structure functions including b_1. In addition, we can also use another convolution description of the virtual nucleon approximation [25–27], which is used for describing the tagged structure functions of the spin-1 deuteron [18].

There is only one type of theoretical calculation in the convolution picture. A basic formalism was shown in Ref. [2], and an updated result is provided in Ref. [4]. Since the deviation from this model is very important for indicating a new hadron-physics mechanism, we need to check its results independently. This is the purpose of this article. In fact, we obtain very different numerical results from the previous theoretical estimate of Ref. [4] as shown in Sec. IV. This work is important for considering the upcoming Thomas Jefferson National Accelerator Facility (JLab) experiments [28,29]. There are also experimental possibilities to investigate the tensor-polarized PDFs and structure functions at Fermilab [8–10] and the future electron-ion collider [30].

We use two types of convolution formalisms for calculating b_1 of the deuteron. One is a basic one in describing the nuclear structure functions as explained, for example, in Refs. [22–24]. The other is the virtual nucleon approximation in Refs. [18,25–27] by considering that the virtual photon interacts with an off shell nucleon and another spectator nucleon is on mass shell. Consequently, the obtained structure function b_1 from both models is compared with the HERMES measurements.

In this article, we first introduce the tensor structure functions b_{1-4} in Sec. II, and convolution formalism for b_1 is explained in Sec. III. Numerical results are shown in Sec. IV, and they are summarized in Sec. V.

II. TENSOR-POLARIZED STRUCTURE FUNCTION b_1

We introduce tensor-polarized structure functions for a spin-1 hadron in a charged-lepton DIS as shown in Fig. 1. The initial and final lepton momenta are ℓ and ℓ', respectively, $q(=\ell - \ell')$ is the momentum transfer, and P is the spin-1 hadron momentum. The cross section is described by a lepton tensor multiplied by the hadron tensor $W_{\mu\nu}$ expressed in terms of eight structure functions as [2,31,32]

$$
\begin{aligned}
W_{\mu\nu}^{\lambda'\lambda}(P,q) &= \frac{1}{4\pi}\int d^4\xi e^{iq\cdot\xi}\langle P,\lambda'|[J_\mu^{em}(\xi),J_\nu^{em}(0)]|P,\lambda\rangle \\
&= -F_1\hat{g}_{\mu\nu} + \frac{F_2}{M\nu}\hat{P}_\mu\hat{P}_\nu + \frac{ig_1}{\nu}\epsilon_{\mu\nu\lambda\sigma}q^\lambda S^\sigma + \frac{ig_2}{M\nu^2}\epsilon_{\mu\nu\lambda\sigma}q^\lambda(P\cdot qS^\sigma - S\cdot qP^\sigma) \\
&\quad - b_1 r_{\mu\nu} + \frac{1}{6}b_2(s_{\mu\nu} + t_{\mu\nu} + u_{\mu\nu}) + \frac{1}{2}b_3(s_{\mu\nu} - u_{\mu\nu}) + \frac{1}{2}b_4(s_{\mu\nu} - t_{\mu\nu}),
\end{aligned}
\tag{1}
$$

where the new tensor-polarized structure functions are b_{1-4}, which do not exist for the spin-1/2 nucleon. The coefficients $r_{\mu\nu}$, $s_{\mu\nu}$, $t_{\mu\nu}$, and $u_{\mu\nu}$ are defined by the spin-1 polarization vector E^μ, hadron and virtual-photon momenta (P,q), and initial and final spin states (λ, λ') as

$$
\begin{aligned}
r_{\mu\nu} &= \frac{1}{\nu^2}\left[q\cdot E^*(\lambda')q\cdot E(\lambda) - \frac{1}{3}\nu^2\kappa\right]\hat{g}_{\mu\nu}, \qquad
s_{\mu\nu} = \frac{2}{\nu^2}\left[q\cdot E^*(\lambda')q\cdot E(\lambda) - \frac{1}{3}\nu^2\kappa\right]\frac{\hat{P}_\mu\hat{P}_\nu}{M\nu}, \\
t_{\mu\nu} &= \frac{1}{2\nu^2}\left[q\cdot E^*(\lambda')\{\hat{P}_\mu\hat{E}_\nu(\lambda) + \hat{P}_\nu\hat{E}_\mu(\lambda)\} + \{\hat{P}_\mu\hat{E}_\nu^*(\lambda') + \hat{P}_\nu\hat{E}_\mu^*(\lambda')\}q\cdot E(\lambda) - \frac{4\nu}{3M}\hat{P}_\mu\hat{P}_\nu\right], \\
u_{\mu\nu} &= \frac{M}{\nu}\left[\hat{E}_\mu^*(\lambda')\hat{E}_\nu(\lambda) + \hat{E}_\nu^*(\lambda')\hat{E}_\mu(\lambda) + \frac{2}{3}\hat{g}_{\mu\nu} - \frac{2}{3M^2}\hat{P}_\mu\hat{P}_\nu\right],
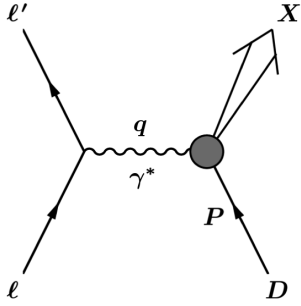\end{aligned}
\tag{2}
$$

FIG. 1.   Charged-lepton DIS from a spin-1 hadron.

where the states λ and λ' are explicitly denoted for describing higher-twist contributions by off diagonal terms with $\lambda' \neq \lambda$ [2]. Here, $\hat{g}_{\mu\nu}$ and $\hat{X}_\mu (= \hat{P}_\mu, \hat{E}_\mu)$ are defined as

$$\hat{g}_{\mu\nu} \equiv g_{\mu\nu} - \frac{q_\mu q_\nu}{q^2}, \qquad \hat{X}_\mu \equiv X_\mu - \frac{X \cdot q}{q^2} q_\mu, \qquad (3)$$

to satisfy the current conservation $q^\mu W_{\mu\nu} = q^\nu W_{\mu\nu} = 0$, M is the hadron mass, ν and Q^2 are defined by $\nu = P \cdot q/M$, $Q^2 = -q^2 > 0$, $\epsilon_{\mu\nu\lambda\sigma}$ is an antisymmetric tensor with the convention $\epsilon_{0123} = +1$, κ is defined by $\kappa = 1 + Q^2/\nu^2$, and S^μ is the spin vector of the spin-1 hadron. The polarization vector satisfies the constraints, $P \cdot E = 0$ and $E^* \cdot E = -1$, and it is taken as the spherical unit vectors [33] for the spin-1 hadron at rest. It is related to the spin vector by

$$(S_{\lambda'\lambda})^\mu = -\frac{i}{M} \epsilon^{\mu\nu\alpha\beta} E_\nu^*(\lambda') E_\alpha(\lambda) P_\beta. \qquad (4)$$

The structure functions b_1 and b_2 are twist-2 structure functions, and they are related to each other by the Callan-Gross-like relation $2x_D b_1 = b_2$ in the Bjorken scaling limit. The functions b_3 and b_4 are twist-4 ones, so that the leading structure functions would be investigated first. In the parton model, b_1 is expressed in terms of the tensor-polarized parton distribution functions $\delta_T f$ as [34]

$$b_1(x, Q^2) = \frac{1}{2} \sum_i e_i^2 [\delta_T q_i(x, Q^2) + \delta_T \bar{q}_i(x, Q^2)],$$

$$\delta_T f(x, Q^2) \equiv f^0(x, Q^2) - \frac{f^{+1}(x, Q^2) + f^{-1}(x, Q^2)}{2}, \qquad (5)$$

where f^λ is an unpolarized parton distribution in the hadron spin state λ, and e_i is the charge of the quark flavor i. The Bjorken scaling variable x defined

$$x = \frac{Q^2}{2M_N \nu}, \qquad (6)$$

where M_N is the nucleon mass, and the scaling variable could be defined as $x_D = Q^2/(2P \cdot q)$ for the deuteron so as to satisfy the kinematical condition $0 < x_D < 1$. For the

fixed-target deuteron, they are related to each other by $x = x_D M/M_N \simeq 2x_D$, so that the range of the Bjorken variable becomes $0 < x \lesssim 2$. So far, the variable x is used for showing experimental data of deuteron structure functions. At this stage, there is no DIS measurement at a large-enough invariant mass, $W^2 > 4$ GeV^2, in the range $1 < x < 2$. The notation for $\delta_T f$ in Eq. (5) indicates that b_1 probes very different spin structure in a hadron. Namely, $\delta_T f$ is the *unpolarized* quark distribution in a tensor-polarized hadron, whereas the polarized structure function g_1 indicates the longitudinally polarized quark distribution in a longitudinally polarized hadron.

A useful guideline for b_1 is expressed as the b_1 sum rule in the parton model [3,21], and it is obtained in the similar way to the Gottfried sum rule [35],

$$\int dx b_1(x) = -\lim_{t \to 0} \frac{5}{24} t F_Q(t)$$
$$+ \frac{1}{9} \int dx [4\delta_T \bar{u}(x) + \delta_T \bar{d}(x) + \delta_T \bar{s}(x)],$$

$$\int \frac{dx}{x} [F_2^p(x) - F_2^n(x)] = \frac{1}{3} + \frac{2}{3} \int dx [\bar{u}(x) - \bar{d}(x)]. \qquad (7)$$

Here, the function $F_Q(t)$ is the electric quadrupole form factor for the spin-1 hadron, so that the first term vanishes: $\lim_{t \to 0} \frac{5}{24} t F_Q(t) = 0$, whereas the first term of the Gottfried sum is finite $(1/3)$. These sums originate from the fact that the valence-quark numbers depend on the quark flavor but not on the hadron spin. As the Gottfried-sum-rule violation indicated the flavor asymmetric distribution $\bar{u}(x) - \bar{d}(x)$, the b_1 sum-rule violation could initiate the studies of finite tensor-polarized antiquark distributions. In fact, the HERMES data in the range $Q^2 > 1$ GeV^2 indicated that it is violated, $\int_{0.02}^{0.85} dx b_1(x) = [0.35 \pm (\text{stat}) \pm 0.18 (\text{syst})] \times 10^{-2}$. This suggestion of finite tensor-polarized antiquark distributions should be tested by polarized proton-deuteron Drell-Yan process at Fermilab or other hadron facilities. Recently, the tensor-polarization asymmetry is theoretically estimated for the Fermilab Drell-Yan experiment [10], and it is considered within the Fermilab E1039 experiment.

Other definition of b_{1-4}: There is another definition of the tensor-polarized structure functions by Edelmann, Piller, and Weise (EPW) [6] and it should not be confused with the one in Eq. (1), which is so far used in this article and for showing numerical results, by Hoodbhoy, Jaffe, and Manohar (HJM) [2]. They introduced structure functions, which we denote as b_{1-3}^{EPW} and Δ^{EPW}, which are not equal to b_{1-4}. Comparing the two hadronic tensors and structure functions functions, we can relate the two sets to each other. For example, the HJM structure function b_1 so far used in our article is related to the EPW functions by

$$\left(1 + \frac{Q^2}{\nu^2}\right) b_1 = b_1^{\text{EPW}} - \frac{\Delta^{\text{EPW}}}{2}. \qquad (8)$$

The structure functions $b_{1,2}$ in the two sets become equal in the scaling limit, and the higher-twist ones are considered equal to zero in the same limit. The function b_1^{EPW} is defined such that the ratio of the following transverse structure functions, $F_{UT_{LL},T}$ and $F_{UU,T}$, defined in Eq. (27), are given by the ratio of b_1^{EPW} and F_1 as shown later in Eq. (34).

III. THEORETICAL FORMALISMS FOR b_1

A. Theory 1: Basic convolution description

The most standard way of calculating nuclear structure functions at medium- and large- x regions ($x > 0.2$) is to use a convolution formalism. A nuclear hadron tensor $W_{\mu\nu}^A$ is given by the nucleonic one $W_{\mu\nu}$ convoluted with a nucleon momentum distribution $S(p)$, which is called the spectral function, in a nucleus [22–24]

$$W_{\mu\nu}^A(P_A, q) = \int d^4 p S(p) W_{\mu\nu}(p, q), \qquad (9)$$

where p and P_A are momenta for the nucleon and nucleus, respectively. As illustrated in Fig. 2, a nucleon is distributed in a nucleus by the spectral function $S(p)$ and a quark is distributed in the nucleon by the distribution function $q(x)$, and the overall nuclear quark distribution is given by the convolution integral of their functions. The spectral function is given by

$$S(p) = \frac{1}{A} \sum_i |\phi_i(\vec{p})|^2 \delta\left(p^0 - M_A + \sqrt{M_{A-i}^2 + \vec{p}^2}\right), \qquad (10)$$

in a simple shell model. Here, M_{A-i} is the mass of a residual one-hole state by removing a nucleon, and $\phi_i(\vec{p})$ is the wave function of the nucleon. The separation energy ε_i is the energy required to remove a nucleon from the state i, and it is expressed by the nuclear mass M_A and the mass M_{A-i} as
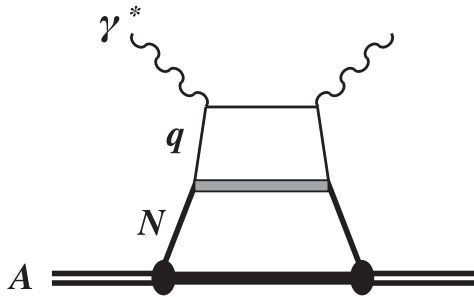

FIG. 2. Convolution description for a structure function of the deuteron. The notations γ^*, q, N, and A indicate the virtual photon, quark, nucleon, and nucleus, respectively.

$$\varepsilon_i = (M_{A-i} + M_N) - M_A. \qquad (11)$$

In our actual calculation for the deuteron, a nonrelativistic relation is used for $\sqrt{M_{A-i}^2 + \vec{p}^2}$, so that the energy conservation by the δ function indicates

$$p^0 = M_N - \varepsilon - \frac{\vec{p}^2}{2M_N}, \qquad (12)$$

where ε is the separation energy for the deuteron. Since the large-momentum contribution decreases significantly due to the deuteron wave function $\phi(p)$, this nonrelativistic approximation does not change the result to a significant amount.

As discussed in Ref. [2], the hadron tensors could be expressed in terms of their helicity amplitudes of the virtual photon as

$$A_{hH,hH}(x, Q^2) = \varepsilon_h^{*\mu} \varepsilon_h^\nu W_{\mu\nu}^D(p_D, q), \qquad (13)$$

for the deuteron and the corresponding one $\hat{A}_{hs,hs}(x, Q^2)$ for the nucleon. The photon polarization vector ε_h^μ is given by

$$\varepsilon_{h=\pm 1}^\mu = \frac{1}{\sqrt{2}}(0, \mp 1, -i, 0),$$

$$\varepsilon_{h=0}^\mu = \frac{1}{\sqrt{Q^2}}(|\vec{q}|, 0, 0, q^0). \qquad (14)$$

Then, the helicity amplitudes are related to the structure function b_1 of the deuteron and F_1 of the nucleon (denoted as F_1^N) by the relations [2,31]

$$b_1 = A_{+0,+0} - \left. \frac{A_{++,++} + A_{+-,+-}}{2} \right|_{\text{LT}},$$

$$F_1^N = \frac{A_{+\uparrow,+\uparrow} + A_{+\downarrow,+\downarrow}}{2}. \qquad (15)$$

We note that the above relation for b_1 is the leading-twist (LT) expression, which is strict only in the scaling limit. We use these relations for estimating the structure function b_1. At this stage, even leading theoretical calculations without higher-twist effects are valuable in comparison with the existing HERMES measurements.

Using these equations, we obtain the convolution expression for the structure function b_1 of the deuteron as

$$b_1(x, Q^2) = \int \frac{dy}{y} \delta_T f(y) F_1^N(x/y, Q^2),$$

$$\delta_T f(y) \equiv f^0(y) - \frac{f^+(y) + f^-(y)}{2}. \qquad (16)$$

Here, the structure function b_1 is defined by the one per nucleon, the light cone momentum distribution is expressed

by the momentum-space wave function of the deuteron $\phi^H(\vec{p})$ as

$$f^H(y) = \int d^3py|\phi^H(\vec{p})|^2\delta\left(y - \frac{E - p_z}{M_N}\right), \quad (17)$$

where the variable y is the momentum fraction defined by

$$y = \frac{Mp \cdot q}{M_N P \cdot q} \simeq \frac{2p^-}{P^-}, \quad (18)$$

where p^- is a light cone momentum $[p^- \equiv (p^0 - p^3)/\sqrt{2}]$. We consider a collinear frame with the photon three momentum along the positive z axis, and consequently the minus component (p^-) of nucleon and deuteron momenta survives as their light-front momentum component, whereas it is p^+ if the z axis is taken as the nucleon momentum. The function F_1^N is defined for the nucleon by the average of the proton and neutron structure functions: $F_1^N = (F_1^p + F_1^n)/2$. Since b_1 is associated with unpolarized quark distributions, the nucleon spin also does not appear in the convolution integral. Namely, the momentum distribution is for the unpolarized nucleon: $f^H(y) \equiv f_\uparrow^H(y) + f_\downarrow^H(y)$ if $f_s^H(y)$ indicates the distribution of the nucleon with the spin state s and the deuteron spin H along the z axis.

The wave function of the deuteron is written as

$$\phi^H(\vec{p}) = \phi_0(p)Y_{00}(\hat{p})\chi_H$$
$$+ \sum_{m_L}\langle 2m_L : 1m_S|1H\rangle\phi_2(p)Y_{2m_L}(\hat{p})\chi_{m_S}, \quad (19)$$

where $\phi_0(p)$ and $\phi_2(p)$ are S- and D-state wave functions with the D-state admixture probability $\int dp\,p^2|\phi_2(p)|^2$. Here, Y_{Lm_L} is the spherical harmonic, $\langle Lm_L : Sm_S|1H\rangle$ is the Clebsch-Gordan coefficient, and χ_{m_S} is the spin wave function. The coordinate-space wave function is written as

$$\psi^H(\vec{r}) = [u_0(r)/r]Y_{00}(\hat{r})\chi_H$$
$$+ \sum_{m_L}\langle 2m_L : 1m_S|1H\rangle[u_2(r)/r]Y_{2m_L}(\hat{r})\chi_{m_S}. \quad (20)$$

Then, the momentum-space wave function is related to the coordinate-space one by $\phi_L(p) = 4\pi i^L \int dr\, r j_L(pr)u_L(r)$, where $j_L(pr)$ is the spherical Bessel function. One may note that the D-state wave function has the negative sign $[\phi_2(p) < 0]$ due to the i^L factor although a different convention $[\phi_2(p) \to -\phi_2(p)$, namely without the i^2 factor] is sometimes used for the D-state wave function. Using the wave function in Eq. (19) for calculating the momentum distribution of Eq. (17), we obtain the tensor distribution of Eq. (16) as

$$\delta_T f(y) = \int d^3py\left[-\frac{3}{4\sqrt{2\pi}}\phi_0(p)\phi_2(p) + \frac{3}{16\pi}|\phi_2(p)|^2\right]$$
$$\times (3\cos^2\theta - 1)\delta\left(y - \frac{p \cdot q}{M_N\nu}\right). \quad (21)$$

For normalizing the momentum distribution, we use the condition of the baryon-number conservation, $\int dy f^H(y) = \int d^3py|\phi^H(\vec{p})|^2 = 1$ [22–24], which is slightly different from the nonrelativistic wave function normalization without the y factor. This issue was discussed in the convolution description for nuclear structure functions, so that the interested reader may look at the articles in Refs. [22–24]. The expression of Eq. (21) is similar to the one given in Ref. [4], which is the updated version of the original convolution formalism in Ref. [2].

The purposes of our work are to study the convolution expression independent from Ref. [4] and to check their numerical result. On the second point, we find very large differences from their b_1 as discussed in Sec. IV. On the formalism, there are some differences. First, our wave function is normalized by the baryon-number conservation including the factor y as it is usually used in the convolution formalism for the nuclear structure functions [22–24]. In Refs. [2,4], the wave function is normalized by $\int dy f(y) = 1$ as written below Eq. (22) of the Hoodbhoy-Jaffe-Manohar paper, in a similar way to satisfy the baryon-number conservation in this work, however, by using a relativistic correction factor $1 + \alpha_3$ with the Dirac spinor. Second, p^0 is defined in the spectral function with the energy-conserving δ function of Eq. (10), which leads to the relation Eq. (12) by the nonrelativistic approximation. However, it is simply assumed as $p^0 = M - \varepsilon + \vec{p}^2/(2M_N)$, where the last kinetic term has the opposite sign, in Refs. [2,4].

For the F_1^N structure function, we use the leading-order (LO) expression with the longitudinal-transverse ratio $R = [(1 + Q^2/\nu^2)F_2^N - 2xF_1^N]/(2xF_1^N)$ as

$$F_1^N(x, Q^2) = \frac{1 + 4M_N^2x^2/Q^2}{2x[1 + R(x, Q^2)]}F_2^N(x, Q^2),$$
$$F_2^N(x, Q^2)_{\text{LO}} = x\sum_i e_i^2[q_i(x, Q^2) + \bar{q}_i(x, Q^2)]_{\text{LO}}. \quad (22)$$

There exists a parton-model expression for F_1^N by the Callan-Gross relation to F_2^N $[F_1^N = F_2^N/(2x)]$ in the Bjorken-scaling limit. However, Eq. (22) is practically used for calculating F_1^N by taking into account the finite longitudinal-transverse ratio. The structure function F_1^N is for the nucleon within the deuteron. We calculated it by neglecting nuclear corrections by the following reasons. First, nuclear modifications are typically within a few percent in F_2 for the deuteron [36]. Furthermore, there is no experimental signature on nuclear modifications of R

[37], although such effects could exist theoretically, for example, by the Fermi motion of nucleons [23]. In any case, nuclear medium effects are considered to be small in the deuteron, so that they are neglected in our numerical estimates.

Using Eqs. (16), (21), and (22), we obtain numerical results for this theoretical model as discussed in Sec. IV. We should note that the leading-twist relation of Eq. (15) is used for obtaining the convolution equation (16), so that its numerical results are not precise at a small Q^2. As for the structure function F_1^N in the convolution integral, we used a realistic one, which corresponds most closely to the one obtained from experiments, in Eq. (22). This choice is also intended for comparison with theory-2 results as mentioned in the end of Sec. III B. Therefore, higher-twist effects are contained in the nucleonic structure-function level, whereas they are neglected in the convolution expression in the theory-1 description. We need to be aware of it in looking at numerical results in Sec. IV.

B. Theory 2: Virtual nucleon approximation

Next, we explain another convolution formalism by using the virtual nucleon approximation. Before stepping into the model, we introduce a general formalism for polarization factors. The density matrix for a spin-1 hadron is written by the spin-polarization vector $\vec{\mathcal{P}}$ and rank-2 spin tensor T_{ij} as [38]

$$\rho = \frac{1}{3}\left[1 + \frac{3}{2}\vec{\mathcal{P}}\cdot\vec{S} + \sqrt{\frac{3}{2}}T_{ij}(S_iS_j + S_jS_i)\right], \quad (23)$$

where $\vec{S}$ is the 3×3 matrix representing the spin operator $\hat{\vec{S}}$ for the spin-1 hadron. The polarization vector $\vec{\mathcal{P}}$ and the rank-2 spin tensor T_{ij} are defined by

$$\vec{\mathcal{P}} = \langle\hat{\vec{S}}\rangle, \qquad T_{ij} = \frac{1}{2}\sqrt{\frac{3}{2}}\left(\langle\hat{S}_i\hat{S}_j + \hat{S}_j\hat{S}_i\rangle - \frac{4}{3}\delta_{ij}\right). \quad (24)$$

The degrees of vector and tensor polarizations are given by $\mathcal{P} = \sqrt{\vec{\mathcal{P}}^2}$ and $T = \sqrt{\sum_{i,j}(T_{i,j})^2}$. If the probabilities of spin states $+1$, 0, and -1 are denoted as p^{+1}, p^0, and p^{-1}, respectively, by taking the z' axis as the quantization axis, the vector and tensor polarizations are

$$\mathcal{P}_{z'} = p^+ - p^-, \qquad T_{z'z'} = \frac{1}{\sqrt{6}}(1 - 3p^0), \quad (25)$$

respectively. We denote this tensor polarization also as

$$\tilde{T}_{\|\|\|} = \frac{1}{\sqrt{6}}(1 - 3p^0). \quad (26)$$

The inclusive cross section of a charged-lepton deep inelastic scattering from a spin-1 target is generally expressed as

$$\frac{d\sigma}{dxdQ^2} = \frac{\pi y^2 \alpha^2}{Q^4(1-\epsilon)}\left[F_{UU,T} + \epsilon F_{UU,L}\right.$$
$$+ T_{\|\|\|}(F_{UT_{LL},T} + \epsilon F_{UT_{LL},L})$$
$$+ T_{\|\perp}\cos\phi_{T_\|}\sqrt{2\epsilon(1+\epsilon)}F_{UT_{LT}}^{\cos\phi_{T_\|}}$$
$$\left. + T_{\perp\perp}\cos(2\phi_{T_\perp})\epsilon F_{UT_{TT}}^{\cos(2\phi_{T_\perp})}\right], \quad (27)$$

in terms of the spin-dependent factors and structure functions [18]. Here, the z axis is taken along the virtual-photon momentum direction $(\vec{q}/|\vec{q}|)$. Then, the polarization factors $T_{\|\|\|}$, $T_{\|\perp}$, and $T_{\perp\perp}$ are related to T_{ij} by the relations $T_{\|\|\|} = T_{zz}$, $T_{\|\perp}\cos\phi_{T_\|} = T_{xz}$, and $T_{\perp\perp}\cos(2\phi_{T_\perp}) = T_{xx} - T_{yy}$ by assigning the angles $\phi_{T_\|}$ and $\phi_{T_\perp}$. Namely, the tensor T is decomposed in three parts: a projection on the longitudinal direction $(T_{\|\|\|})$, a projection on the transverse space $(T_{\perp\perp})$, and a mixed projection $(T_{\|\perp})$, where longitudinal and transverse are relative to $\vec{q}$. The angle $\phi_{T_\|}$ is the azimuthal angle of the transverse part of the mixed projection, and the angle $\phi_{T_\perp}$ is the azimuthal angle in the transverse space of the projection. If the deuteron is polarized along the virtual photon direction, only $T_{\|\|\|}$ is nonzero and given by Eq. (26). If the deuteron is polarized along the lepton-beam axis, we have $\phi_{T_\|} = \phi_{T_\perp} = 0$, and the remaining polarization factors in Eq. (27) can be related to $\tilde{T}_{\|\|\|}$ of Eq. (26) through the transformation properties of the density matrix under rotations as follows:

$$T_{\|\|\|} = \frac{1}{4}[1 + 3\cos(2\theta_q)]\tilde{T}_{\|\|\|}, \qquad T_{\|\perp} = \frac{3}{4}\sin(2\theta_q)\tilde{T}_{\|\|\|},$$
$$T_{\perp\perp} = \frac{3}{4}[1 - \cos(2\theta_q)]\tilde{T}_{\|\|\|}, \quad (28)$$

where θ_q is the angle between the lepton-beam (z') and virtual-photon (z) direction. The variables y and γ are defined by the spin-1 hadron momentum P, its mass M, the initial lepton momentum ℓ, the momentum transfer q, and Q^2 as

$$y = \frac{P\cdot q}{P\cdot \ell}, \qquad \gamma = \frac{\sqrt{Q^2}}{\nu} = \sqrt{1-\kappa}. \quad (29)$$

The factor ϵ indicates the degree of the longitudinal polarization of the virtual photon as it appears in front of the longitudinal structure function $F_{UU,L}$, and it is given by

$$\epsilon = \frac{1}{1 + (1 + \nu^2/Q^2)\tan^2(\theta/2)}, \quad (30)$$

where θ is the scattering angle of the charged lepton. The six structure functions in Eq. (27) can be written by the virtual photon helicity amplitudes of the hadronic tensor in Eq. (13). Then, the tensor polarized structure functions, which are used to calculate b_1 below, are expressed by the photon helicity amplitudes as

$$F_{UT_{LL},L} = \frac{4}{\sqrt{6}}(A_{+0,+0} - A_{00,00}),$$

$$F_{UT_{LL},T} = \frac{2}{\sqrt{6}}(A_{++,++} - 2A_{+0,+0} + A_{+-,+-}),$$

$$F_{UT_{LT}}^{\cos\phi_{T_\parallel}} = -\frac{4}{\sqrt{6}}\Re e(A_{+0,0+} - A_{+-,00}),$$

$$F_{UT_{TT}}^{\cos(2\phi_{T_\perp})} = -\sqrt{\frac{2}{3}}\Re eA_{+-,-+}. \tag{31}$$

Using the expression of Eq. (1) for the hadron tensor in terms of the polarized structure functions b_{1-4} and the helicity amplitude definition of Eq. (13), we obtain [18]

$$F_{UT_{LL},L} = \frac{1}{x_D}\sqrt{\frac{2}{3}}\left[2(1+\gamma^2)x_Db_1 - (1+\gamma^2)^2\left(\frac{1}{3}b_2 + b_3 + b_4\right)\right.$$
$$\left. - (1+\gamma^2)\left(\frac{1}{3}b_2 - b_4\right) - \left(\frac{1}{3}b_2 - b_3\right)\right],$$

$$F_{UT_{LL},T} = -\frac{1}{x_D}\sqrt{\frac{2}{3}}\left[2(1+\gamma^2)x_Db_1 - \gamma^2\left(\frac{1}{6}b_2 - \frac{1}{2}b_3\right)\right],$$

$$F_{UT_{LT}}^{\cos\phi_{T_\parallel}} = -\sqrt{\frac{2}{3}}\frac{\gamma}{2x_D}\left[(1+\gamma^2)\left(\frac{1}{3}b_2 - b_4\right) + \left(\frac{2}{3}b_2 - 2b_3\right)\right],$$

$$F_{UT_{TT}}^{\cos(2\phi_{T_\perp})} = -\sqrt{\frac{2}{3}}\frac{\gamma^2}{x_D}\left(\frac{1}{6}b_2 - \frac{1}{2}b_3\right). \tag{32}$$

Therefore, the b_1 is written through the structure functions $F_{UT_{LL},T}$ and $F_{UT_{TT}}$ as

$$b_1 = -\frac{1}{1+\gamma^2}\sqrt{\frac{3}{8}}[F_{UT_{LL},T} + F_{UT_{TT}}^{\cos(2\phi_{T_\perp})}]. \tag{33}$$

We also show the relation between these structure functions and the EPW function b_1^{EPW}, which is related by the ratio of transverse structure functions, as

$$\sqrt{\frac{2}{3}}\frac{F_{UT_{LL},T}}{F_{UU,T}} = \frac{A_{++,++} - 2A_{+0,+0} + A_{+-,+-}}{A_{++,++} + A_{+0,+0} + A_{+-,+-}}$$
$$= -\frac{2}{3}\frac{b_1^{\text{EPW}}}{F_1}. \tag{34}$$

This equality is not valid with the HJM b_1 because the structure functions b_2, b_3 also contribute to $F_{UT_{LL},T}$ as shown in Eq. (32).

Next, we explain how to calculate the structure functions $F_{UT_{LL},T}$ and $F_{UT_{TT}}$ for the deuteron by the virtual nucleon approximation (VNA), which considers the np component of the light-front deuteron wave function. As shown in Fig. 3, the virtual photon interacts with one nucleon which is off the mass shell in the DIS reaction, while the second noninteracting "spectator" is assumed to be on its mass
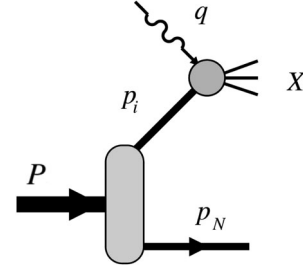

FIG. 3. Impulse approximation diagram in the VNA. For the inclusive reaction, we integrate over the phase space of the spectator nucleon.

shell. Then, the inclusive structure functions in the impulse approximation are obtained by integrating over all possible spectator momenta $\vec{p}_N$.

In the following, we explain the outline for deriving the tensor polarized structure functions in the light-front formulation of the VNA. In Fig. 3, P, p_i, and p_N are momenta for the deuteron ($P = p_i + p_N$), the struck nucleon, and the on shell spectator, respectively. The convolution approach for the symmetric part of the hadron tensor is given in the VNA model for the deuteron as [18]

$$W_{\mu\nu}^{\lambda'\lambda}(P,q) = 4(2\pi)^3\int d\Gamma_N\frac{\alpha_N}{\alpha_i}W_{\mu\nu}^N(p_i,q)\rho_D(\lambda',\lambda), \tag{35}$$

where $W_{\mu\nu}^N$ is the hadron tensor for the nucleon and $d\Gamma_N$ is the Lorentz invariant phase space for the spectator nucleon. We note that only the symmetric term of $W_{\mu\nu}^{\lambda'\lambda}$ under the exchange $\mu \leftrightarrow \nu$ is relevant for the tensor structure functions b_{1-4}. The factor $4(2\pi)^3$ arises in defining the deuteron light cone wave function, which is shown later in Eqs. (39) and (41), and the factor α_N/α_i appears because the hadron tensor $W_{\mu\nu}$ is for the nucleon with momentum p_i instead of the nucleon at rest [18]. Here, the light cone momentum fractions are defined for the interacting (i) and spectator (N) nucleons as

$$\alpha_i = \frac{2p_i^-}{P^-}, \qquad \alpha_N = \frac{2p_N^-}{P^-} = 2 - \alpha_i. \tag{36}$$

Next, we define the relative momentum $\vec{k}$ of two nucleons by [39]

$$k = \sqrt{E_k^2 - M_N^2}, \qquad E_k^2 = \frac{m_N^2 + \vec{k}^{\perp 2}}{\alpha_i(2-\alpha_i)},$$
$$k^3 = (1-\alpha_i)E_k, \qquad \vec{k}^\perp = \vec{p}_i^\perp + \frac{\alpha_i}{2}\vec{P}^\perp. \tag{37}$$

The momentum k corresponds with the relative momentum of the free two nucleon state with identical light-front momentum components (P^-, $P^\perp$) as the deuteron, and the

overlap of this state with the deuteron defines the deuteron light-front wave function. The spectator nucleon phase-space element can be written with the variables of Eqs. (36) and (37) as

$$d\Gamma_N = \frac{d^3 p_N}{2E_{p_N}(2\pi)^3} = \frac{d\alpha_i d\vec{p}_i^{\perp}}{2\alpha_i(2\pi)^3} = \frac{\alpha_i d^3 \vec{k}}{2E_k(2\pi)^3}. \quad (38)$$

In Eq. (35), the deuteron density $\rho_D(\lambda', \lambda)$ is defined by the light-front deuteron wave function $\Psi_\lambda^D(\vec{k}, \lambda'_N, \lambda_N)$

$$\rho_D(\lambda', \lambda) = \sum_{\lambda_N, \lambda'_N} \frac{[\Psi_{\lambda'}^D(\vec{k}, \lambda'_N, \lambda_N)]^\dagger \Psi_\lambda^D(\vec{k}, \lambda'_N, \lambda_N)}{\alpha_N \alpha_i}, \quad (39)$$

and it is expressed as [18,25–27]

$$\Psi_\lambda^D(\vec{k}, \lambda_1, \lambda_2) = \sqrt{E_k} \sum_{\lambda'_1, \lambda'_2} \mathcal{D}_{\lambda_1 \lambda'_1}^{\frac{1}{2}}[R(k_1/m_N)]$$

$$\times \mathcal{D}_{\lambda_2 \lambda'_2}^{\frac{1}{2}}[R(k_2/m_N)] \sum_{\substack{l=0,2 \\ \lambda_l \lambda_S}} \langle l\lambda_l : S\lambda_S | j\lambda \rangle$$

$$\times \langle s_1 \lambda'_1 : s_2 \lambda'_2 | 1\lambda_S \rangle Y_{l\lambda_l}(\Omega_{\mathbf{k}})(-i)^l \phi_l(k), \quad (40)$$

where $\mathcal{D}_{\lambda\lambda'}^{\frac{1}{2}}$ is the rotation matrix and $\phi_i(k)$ is the deuteron wave function with the orbital angular momentum l. The notation R indicates the Melosh rotation, which relates canonical and light-front quantized spinors, and the nucleon momenta $[k_1 = (E_k, \vec{k}), k_2 = (E_k, -\vec{k})]$. The wave functions are approximated by the nonrelativistic ones $\phi_0(k) = U(k)$ and $(-i)^2\phi_2(k) = W(k)$. It is important to note, as discussed below Eq. (21), that the deuteron light-front wave function of Eq. (40) satisfies the baryon and momentum sum rules [18,25]

$$\sum_{\lambda_1, \lambda_2} \int \frac{d\alpha_i d\vec{k}^\perp}{\alpha_i(2 - \alpha_i)} |\Psi_\lambda^D(\alpha_i, \vec{k}^\perp, \lambda_1, \lambda_2)|^2 = 1,$$

$$\sum_{\lambda_1, \lambda_2} \int \frac{d\alpha_i d\vec{k}^\perp}{\alpha_i(2 - \alpha_i)} \alpha_i |\Psi_\lambda^D(\alpha_i, \vec{k}^\perp, \lambda_1, \lambda_2)|^2 = 1. \quad (41)$$

Using the convolution equation (35) by the VNA model with the deuteron wave function (40), the helicity amplitudes (13), and their relations to $F_{UT_{LL},L}$ and $F_{UT_{LL},T}$ in Eq. (31), we obtain the structure functions in the VNA convolution model as

$$F_{UT_{LL},T} = -\int \frac{k^2}{\alpha_i} dk d(\cos\theta_k) \left[F_1^N(x_i, Q^2) \right.$$

$$\left. - \frac{T^2}{2p_i \cdot q} F_2^N(x_i, Q^2) \right]$$

$$\times \sqrt{\frac{3}{2}} \left[\frac{U(k)W(k)}{\sqrt{2}} + \frac{W(k)^2}{4} \right] [3\cos(2\theta_k) + 1],$$

$$F_{UT_{TT}}^{\cos(2\phi_{T_\perp})} = -\int \frac{k^2}{\alpha_i} dk d(\cos\theta_k) \frac{-T^2}{2p_i \cdot q} F_2^N(x_i, Q^2)$$

$$\times \sqrt{\frac{3}{2}} \left[\frac{U(k)W(k)}{\sqrt{2}} + \frac{W(k)^2}{4} \right] \sin^2\theta_k, \quad (42)$$

where the structure functions F_1^N and F_2^N are defined by the averages of the proton and neutron functions as defined in Sec. III A and θ_k is the angle between $\vec{k}$ and $\vec{q}$. Here, T^μ and L^μ are defined by

$$T^\mu = p_N^\mu + \frac{p_N \cdot q}{Q^2} q^\mu - \frac{p_N \cdot L}{L^2} L^\mu, \quad L^\mu = P^\mu + \frac{P \cdot q}{Q^2} q^\mu. \quad (43)$$

The nucleon structure functions F_1^N and F_2^N are evaluated at $x_i = Q^2/(2p_i \cdot q) \simeq x/\alpha_i$. Substituting the structure functions of Eq. (42) into Eq. (33), we finally obtain the expression for b_1 in the VNA model,

$$b_1(x, Q^2) = \frac{3}{4(1 + \gamma^2)} \int \frac{k^2}{\alpha_i} dk d(\cos\theta_k)$$

$$\times \left[F_1^N(x_i, Q^2)(6\cos^2\theta_k - 2) \right.$$

$$\left. - \frac{T^2}{2p_i \cdot q} F_2^N(x_i, Q^2)(5\cos^2\theta_k - 1) \right]$$

$$\times \left[\frac{U(k)W(k)}{\sqrt{2}} + \frac{W(k)^2}{4} \right]. \quad (44)$$

In deriving this expression of the theory 2, the Bjorken scaling limit is not taken and the higher-twist effects are contained as it is clear by the additional term of F_2^N in comparison with Eq. (16) of the theory 1. Because of the higher-twist effects included, for self-consistency, the theory 2 should include nucleon structure functions that also contain higher-twist effects. For the purpose of the comparison with the theory 1 in evaluating only higher-twist effects originating from the nuclear part, we use the same nucleon structure function used in theory 1 [Eq. (22)].

C. Tensor-polarization asymmetry A_{zz} and structure function b_1

In the unpolarized charged-lepton DIS from the polarized deuteron like the HERMES experiment [20], the cross section with target polarization along the beam direction is written as

TABLE I.   Theory-2 calculations of the four tensor-polarized structure functions for kinematics of the HERMES b_1 data [20].

x	Q^2 (GeV^2)	$b_1(10^{-4})$	$b_2(10^{-5})$	$b_3(10^{-3})$	$b_4(10^{-3})$	$b_2/(2x_Db_1)$	γ
0.012	0.51	2.81	0.264	−1.34	5.06	0.783	0.0315
0.032	1.06	6.92	1.97	−1.87	7.51	0.890	0.0583
0.063	1.65	3.50	0.265	−2.02	7.96	0.120	0.0920
0.128	2.33	−1.80	−7.38	−2.13	7.49	3.20	0.157
0.248	3.11	−8.39	−28.1	−2.09	4.58	1.35	0.264
0.452	4.69	−6.18	−21.7	−1.11	−0.58	0.777	0.392

$$\frac{d\sigma}{dxdQ^2} = \frac{d\sigma^U}{dxdQ^2}\left(1 + \frac{1}{2}P_{zz}A_{zz}\right), \qquad (45)$$

where $d\sigma^U/dxdQ^2$ is the unpolarized cross section, and P_{zz} is related to the density matrix variables defined in the beginning of Sec. III B as

$$P_{zz} = \sqrt{6}\tilde{T}_{zz} = p^+ + p^- - 2p^0. \qquad (46)$$

Comparing Eq. (45) with Eq. (27), we can write the tensor asymmetry A_{zz} as

$$A_{zz} = \frac{2\sigma^+ - 2\sigma^0}{2\sigma^+ + \sigma^0} = \frac{\sqrt{2}}{4\sqrt{3}(F_{UU,T} + \epsilon F_{UU,L})}$$
$$\times \left\{[1 + 3\cos(2\theta_q)](F_{UT_{LL},T} + \epsilon F_{UT_{LL},L})\right.$$
$$+ 3\sin(2\theta_q)\sqrt{2\epsilon(1+\epsilon)}F_{UT_{LT}}^{\cos\phi_{T_\parallel}}$$
$$\left. + 3[1 - \cos(2\theta_q)]\epsilon F_{UT_{TT}}^{\cos 2\phi_{T_\perp}}\right\}, \qquad (47)$$

where σ^i is the cross section with the target polarization i along the beam (z' axis) and we took $\sigma^+ = \sigma^-$ because of the parity invariance.

In the HERMES analysis, b_1 was then extracted from A_{zz} using

$$A_{zz} = -\frac{2}{3}\frac{b_1}{F_1}. \qquad (48)$$

This equation is correct as an equality if the following two conditions are satisfied.

(1) The deuteron is polarized along the photon direction, namely $\theta_q = 0$.

(2) The Bjorken scaling limit ($Q^2 \to \infty$, x finite, $\gamma \to 0$) is taken. It implies the Callan-Gross relations for the structure functions ($2x_DF_1 = F_2$, $2x_Db_1 = b_2$) and neglect of the higher-twist structure functions $b_{3,4}$.

This can be seen by putting $\theta_q = 0$ in Eq. (47). The surviving structure functions in the scaling limit after applying the Callan-Gross relations become

$$F_{UT_{LL},T} = -2\sqrt{\frac{2}{3}}b_1, \qquad F_{UT_{LL},L} = 0,$$
$$F_{UU,T} = 2F_1, \qquad F_{UU,L} = 0, \qquad (49)$$

which leads to Eq. (48). The theory 2 includes higher-twist corrections and can test the above assumptions. According to our estimate, there are significant higher-twist effects, so that the Callan-Gross relations are not satisfied and the functions $b_{3,4}$ are not very small in comparison with the leading ones $b_{1,2}$ as shown in Table I. These observations and the value of γ for the HERMES kinematics indicate that including higher-twist effects might be needed for an improved extraction of b_1.

IV. RESULTS

In showing our numerical results on b_1 in the convolution picture, we need to choose (1) a deuteron wave function, (2) parton distribution functions (PDFs), and (3) a longitudinal-transverse structure function ratio. Here, the CD-Bonn wave function is used for the deuteron [40], the MSTW2008 (Martin-Stirling-Thorne-Watt, 2008) leading-order (LO) parametrization for the PDFs [41], and the SLAC-R1998 parametrization for the longitudinal-transverse ratio R [42]. We also tested other wave functions and parametrizations, but numerical results do not change by a significant amount. There is a source of the uncertainty due to our knowledge of the high-momentum part of the deuteron wave function, and it reveals itself at $x > 0.8$ kinematics. The experimental separation energy of the deuteron 2.22457 MeV [43] is used in our numerical evaluation.

In Fig. 4, the calculated functions xb_1 are shown for the SD interference term ($\propto \phi_0\phi_2$), DD term ($\propto |\phi_2|^2$), and their summation at $Q^2 = 2.5$ GeV^2 by using the two convolution descriptions in Eqs. (16) and (44). This Q^2 scale is taken because of a later comparison with the HERMES data, where the Q^2 average is $Q^2 = 2.5$ GeV^2. The SD contribution is larger than the DD one; however, the DD term is not small as suggested by the magnitude of the D-state admixture of 4.85% [40]. It indicates that high-momentum components of the deuteron wave functions play an important role in the standard convolution description for b_1.
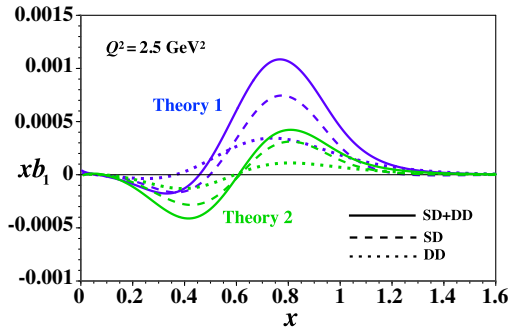
FIG. 4. The structure function b_1 calculated by the two convolution descriptions of Eqs. (16) and (44) at $Q^2 = 2.5$ GeV^2. The dashed, dotted, and solid curves indicate contributions to xb_1 from the SD term, DD term, and their summation. Two sets of theory curves are shown for the theory 1 and theory 2.

FIG. 5. Q^2 dependence of the structure function b_1 by the two convolution descriptions of Eqs. (16) and (44) at $Q^2 = 1.0, 2.5,$ and 5.0 GeV^2. The dashed, dotted, and solid curves indicate contributions to xb_1 from the SD term, DD term, and their summation.

Furthermore, the overall sign of the SD term is opposite to the previous estimate in Ref. [4]. Our convolution formalisms are similar to the one in Ref. [4]; however, the SD term is completely different even in sign. Since the SD contribution is the dominant term, this finding is important for future studies for an experimental comparison and in considering possible theoretical mechanisms of the tensor polarization in the parton level.

In addition, it is noteworthy to find the distribution at $x > 1$, whereas it vanishes according to the analysis of Ref. [4]. However, this region will be dominated by quasielastic scattering at moderate Q^2, and it will require the subtraction of this contribution for the DIS analysis. Since the Bjorken x is defined by the same definition as Eq. (6) in the convolution equations of Refs. [2,4], although it seems to be defined by $x = Q^2/(2M\nu)$ with the deuteron mass M in the beginning of the Hoodbhoy-Jaffe-Manohar paper, the function b_1 should be finite even at $x > 1$. In fact, the upper limit of their convolution integral is $y_{max} = 2$. We could not figure out the reason why they do not have a b_1 distribution at $x > 1$ in Ref. [4].

We used two theoretical models. They are similar but there are some differences. First, the theory 2 in Eq. (44) includes other terms like F_2 in the convolution integral as a higher-twist contribution. There are also differences in kinematical treatments as shown in Eqs. (16) and (44). It suggests that b_1 is sensitive to dynamical details for describing the deuteron. There exist significant differences between the two model predictions, and their possible sources should be discussed. First, the differences partly come from the higher-twist effects, as it is clear from the large differences at $Q^2 = 1$ GeV^2 and also from Table I. To remove such effects, we took the scaling limit $\gamma \to 0$ in the theory 2, and both results become similar. However, a complete agreement was not obtained even in this limit, and the remaining differences come from the slightly different normalizations and relativistic treatments for the deuteron wave functions.
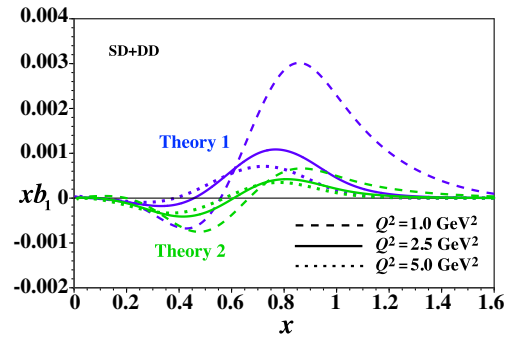
The Q^2 dependence of b_1 is shown in Fig. 5 by taking $Q^2 = 1.0, 2.5,$ and 5.0 GeV^2 in the convolution models. There are significant variations in b_1 in the region 1 GeV$^2 < Q^2 < 5$ GeV^2. This fact also indicates that b_1 is sensitive to dynamical aspects of the hadron structure. There are large differences between theory 1 and theory 2 at $Q^2 = 1$ GeV^2, they are mainly due to the higher-twist effects which are significant at small Q^2.

Next, we compare our total contribution from the SD and DD terms with the HERMES measurement on b_1. In Fig. 6, our xb_1 curves are shown at $Q^2 = 2.5$ GeV^2 for comparison with the HERMES data because the average HERMES scale is $Q^2 = 2.5$ GeV^2. In general, the magnitude of xb_1 is much smaller than the HERMES data at $x < 0.5$, which means that the differences cannot be explained by the conventional deuteron model, and new hadron physics, at least beyond the current standard convolution description, is possibly needed for their interpretation. Because the b_1 is sensitive to the D state, and it is distributed at a relative large x, it is worthwhile to look at resonance effects, which could persist even in the deep inelastic region
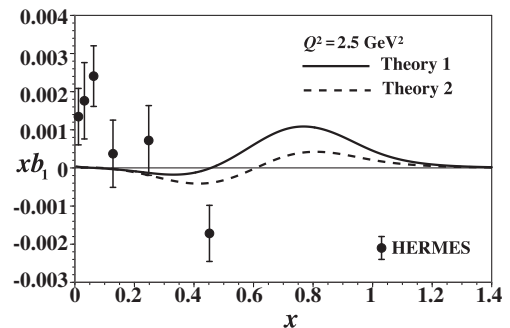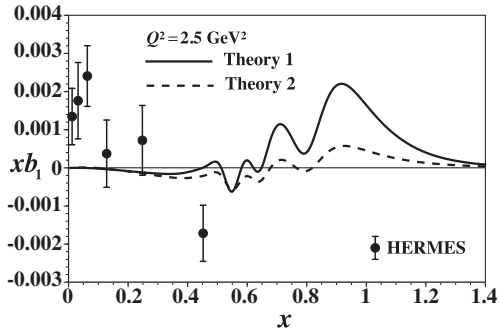

FIG. 6. Calculated structure functions are compared with HERMES experimental data. The solid and dashed curves indicate the functions xb_1 for theory 1 and theory 2, respectively, $Q^2 = 2.5$ GeV^2. Here, the MSTW2008 PDFs are used as they are used in Figs. 4 and 5.

FIG. 7. Calculated structure functions are compared with HERMES experimental data. The solid and dashed curves indicate the functions xb_1 for theory 1 and theory 2, respectively, $Q^2 = 2.5$ GeV^2. The Bodek *et al.* structure functions [44] are used instead of the MSTW2008 in Fig. 6. The other conditions are same as the ones in Fig. 6.

($W^2 \geq 4$ GeV^2) at a Q^2 of a few GeV^2. In order to investigate such effects, we take the structure-function parametrization of Bodek *et al.* in Ref. [44] and show b_1 in Fig. 7. At $x > 0.5$, an interesting bumpy resonance structure appears in b_1 according to the convolution picture. As the quark-hadron duality indicates [45], if the bumpy functions are averaged and they are approximated by smooth curves, they roughly agree with the b_1 functions in Fig. 6.

We reiterate the major points of our results.

(1) Our convolution results for b_1 are numerically very different from the ones in Ref. [4], especially in the SD contribution, although the theoretical formalisms are similar.

(2) There are finite distributions in b_1 even at $x > 1$, whereas there is no distribution in Ref. [4].

(3) Our convolution calculations for b_1 by the standard deuteron picture are very different from the HERMES measurement. It could suggest a new hadron-physics mechanism for interpreting the differences.

Fortunately, a JLab experiment was approved for measuring b_1 accurately at a medium x [28], and also an experiment to measure the tensor-polarization asymmetry A_{zz} at a large x is possible [29], so that the situation should become much clearer in a few years. There is also a possibility to measure the tensor-polarized antiquark distributions in a proton-deuteron Drell-Yan process with the tensor-polarized deuteron target at Fermilab [8–10]. Furthermore, it should be an interesting topic to investigate b_1 at the future electron-ion-collider project [30] and other hadron facilities such as Brookhaven National

Laboratory-RHIC, CERN-COMPASS, Japan Proton Accelerator Research Complex [46], Gesellschaft für Schwerionenforschung-Facility for Antiproton and Ion Research, and Institute for High Energy Physics in Russia. The structure function b_1 could be also investigated at the International Linear Collider (ILC) if a fixed-target experiment becomes possible in the similar way with the TESLA-N project [47].

V. SUMMARY

We calculated the tensor-polarized structure function b_1 for the spin-1 deuteron in the standard convolution description. The structure function b_1 is given by the tensor-polarized light cone momentum distribution for the nucleon convoluted with the unpolarized structure function of the nucleon. Two convolution models are used for evaluating b_1. One is a basic convolution model, and the other is the VNA model. Our numerical results indicate that these standard theoretical predications are much different from the HERMES measurements. Furthermore, significantly large distributions are predicted, at a large x ($x > 0.8$) and even at an extremely large x ($x > 1$). Since our results are very different from the HERMES measurement, new hadronic mechanisms could be needed for interpreting the data although there is still some room to improve the differences due to the higher-twist effects and the experimental extraction of b_1 from A_{zz}. The HERMES data have large uncertainties; however, upcoming JLab experimental measurements will improve on the size of the errors. In addition, there are experimental possibilities at Fermilab, EIC, and other facilities to investigate the tensor-polarized structure functions. It is now a good opportunity to understand the tensor structure in terms of quark and gluon degrees of freedom. Obviously, we need further theoretical studies on b_1 and other spin-1 structure functions possibly by including exotic mechanisms.

ACKNOWLEDGMENTS

[1] L. L. Frankfurt and M. I. Strikman, Nucl. Phys. **A405**, 557 (1983).

[2] P. Hoodbhoy, R. L. Jaffe, and A. Manohar, Nucl. Phys. **B312**, 571 (1989); R. L. Jaffe and A. Manohar, Nucl. Phys. **B321**, 343 (1989).

[3] F. E. Close and S. Kumano, Phys. Rev. D **42**, 2377 (1990); The sum rule is based on the parton model explained in R. P. Feynman, *Photon-Hadron Interactions* (Westview press, Boulder, 1998).

[4] H. Khan and P. Hoodbhoy, Phys. Rev. C **44**, 1219 (1991).

[5] N. N. Nikolaev and W. Schäfer, Phys. Lett. B **398**, 245 (1997); **407**, 453(E) (1997); K. Bora and R. L. Jaffe, Phys. Rev. D **57**, 6906 (1998).

[6] J. Edelmann, G. Piller, and W. Weise, Z. Phys. A **357**, 129 (1997).

[7] G. A. Miller, Phys. Rev. C **89**, 045203 (2014).

[8] S. Hino and S. Kumano, Phys. Rev. D **59**, 094026 (1999); **60**, 054018 (1999); S. Kumano and M. Miyama, Phys. Lett. B **479**, 149 (2000).

[9] S. Kumano and Qin-Tao Song, Phys. Rev. D **94**, 054022 (2016).

[10] Fermilab E1039 experiment, Letter of Intent Report No. P1039, 2013, https://www.fnal.gov/directorate/program_planning/June2013PACPublic/P-1039_LOI_polarized_DY.pdf; X. Jiang, D. Keller, A. Klein, and K. Nakano (private communication); For the on-going Fermilab E-906/SeaQuest experiment, see http://www.phy.anl.gov/mep/drell-yan/.

[11] A. Bacchetta and P. J. Mulders, Phys. Rev. D **62**, 114004 (2000).

[12] A. Schäfer, L. Szymanowski, and O. V. Teryaev, Phys. Lett. B **464**, 94 (1999); K.-B. Chen, W.-H. Yang, S.-Y Wei, and Z.-T Liang, Phys. Rev. D **94**, 034003 (2016).

[13] E. R. Berger, F. Cano, M. Diehl, and B. Pire, Phys. Rev. Lett. **87**, 142302 (2001); A. Kirchner and D. Mueller, Eur. Phys. J. C **32**, 347 (2003); M. Diehl, Phys. Rep. **388**, 41 (2003); F. Cano and B. Pire, Eur. Phys. J. A **19**, 423 (2004); A. V. Belitsky and A. V. Radyushkin, Phys. Rep. **418**, 1 (2005).

[14] W. Detmold, Phys. Lett. B **632**, 261 (2006).

[15] V. Dmitrasinovic, Phys. Rev. D **54**, 1237 (1996).

[16] C. Best, M. Göckeler, R. Horsley, E.-M. Ilgenfritz, H. Perlt, P. Rakow, A. Schäfer, G. Schierholz, A. Schiller, and S. Schramm, Phys. Rev. D **56**, 2743 (1997).

[17] S. K. Taneja, K. Kathuria, S. Liuti, and G. R. Goldstein, Phys. Rev. D **86**, 036008 (2012).

[18] W. Cosyn, M. Sargsian, and C. Weiss, Proc. Sci., DIS2016 (**2016**) 210; (to be published).

[19] R. L. Jaffe and A. Manohar, Phys. Lett. B **223**, 218 (1989); J. P. Ma, C. Wang, and G. P. Zhang, arXiv:1306.6693; W. Detmold et al., Letter of Intent Report No. LOI12-14-001 to Jefferson Lab PAC 42 (2014), https://www.jlab.org/exp_prog/proposals/14prop.html; W. Detmold and P. E. Shanahan, Phys. Rev. D **94**, 014507 (2016).

[20] A. Airapetian et al. (HERMES Collaboration), Phys. Rev. Lett. **95**, 242001 (2005).

[21] S. Kumano, Phys. Rev. D **82**, 017501 (2010).

[22] G. L. Li, K. F. Liu, and G. E. Brown, Phys. Lett. B **213**, 531 (1988); S. Kumano and F. E. Close, Phys. Rev. C **41**, 1855 (1990); M. M. Sargsian, S. Simula, and M. I. Strikman, Phys. Rev. C **66**, 024001 (2002); C. Ciofi degli Atti, L. L. Frankfurt, L. P. Kaptari, and M. I. Strikman, Phys. Rev. C **76**, 055206 (2007); M. Hirai, S. Kumano, K. Saito, and T. Watanabe, Phys. Rev. C **83**, 035202 (2011).

[23] M. Ericson and S. Kumano, Phys. Rev. C **67**, 022201 (2003).

[24] For example, see D. F. Geesaman, K. Saito, and A. W. Thomas, Annu. Rev. Nucl. Part. Sci. **45**, 337 (1995); R. G. Roberts, *The Structure of the Nucleon* (Cambridge University Press, Cambridge, England, 1993), p. 8, 144.

[25] L. L. Frankfurt and M. I. Strikman, Phys. Rep. **76**, 215 (1981).

[26] B. D. Keister and W. Polyzou, Adv. Nucl. Phys. **20**, 225 (1991).

[27] W. Cosyn and M. Sargsian, Phys. Rev. C **84**, 014601 (2011); W. Cosyn, W. Melnitchouk, and M. Sargsian, Phys. Rev. C **89**, 014612 (2014).

[28] Proposal to Jefferson Lab PAC-38 (Report No. PR12-11-110), J.-P. Chen et al. (2011), https://www.jlab.org/exp_prog/proposals/11prop.html.

[29] W. Cosyn and M. Sargsian, J. Phys. Conf. Ser. **543**, 012006 (2014); M. M. Sargsian and M. I. Strikman, J. Phys. Conf. Ser. **543**, 012009 (2014); E. Long, J. Phys. Conf. Ser. **543**, 012010 (2014); T. Badman et al., Letter of Intent Report No. LOI12-14-002 to Jefferson Lab PAC42, https://www.jlab.org/exp_prog/proposals/14prop.html.

[30] W. Cosyn et al., J. Phys. Conf. Ser. **543**, 012007 (2014); N. Kalantarians, J. Phys. Conf. Ser. **543**, 012008 (2014); D. Boer et al., arXiv:1108.1713 (unpublished); A. Accardi et al., Eur. Phys. J. A **52**, 268 (2016); J. L. Abelleira Fernandez et al. J. Phys. G **39**, 075001 (2012).

[31] T.-Y. Kimura and S. Kumano, Phys. Rev. D **78**, 117505 (2008).

[32] S. Kumano, J. Phys. Conf. Ser. **543**, 012001 (2014).

[33] A. R. Edmond, *Angular Momentum in Quantum Mechanics* (Princeton University Press, Princeton, 1974).

[34] The overall factor $1/2$ is introduced in b_1 as it is used in F_1 and g_1 in expressing them by the unpolarized or longitudinally polarized PDFs.

[35] S. Kumano, Phys. Rep. **303**, 183 (1998); G. T. Garvey and J.-C. Peng, Prog. Part. Nucl. Phys. **47**, 203 (2001); J.-C. Peng and J.-W. Qiu, Prog. Part. Nucl. Phys. **76**, 43 (2014).

[36] M. Hirai, S. Kumano, and M. Miyama, Phys. Rev. D **64**, 034003 (2001); M. Hirai, S. Kumano, and T.-H. Nagai, Phys. Rev. C **70**, 044905 (2004); **76**, 065207 (2007).

[37] K. Ackerstaff et al. (HERMES Collaboration), Phys. Lett. B **475**, 386 (2000); **567**, 339(E) (2003).

[38] E. Leader, *Spin in Particle Physics* (Cambridge University Press, Cambridge, 2005).

[39] See Eq. (2.21) of Ref. [25].

[40] R. Machleidt, Phys. Rev. C **63**, 024001 (2001).

[41] A. D. Martin, W. J. Stirling, R. S. Thorne, and G. Watt, Eur. Phys. J. C **63**, 189 (2009).

[42] K. Abe et al. (E143 Collaboration), Phys. Lett. B **452**, 194 (1999).

[43] G. Audia, A. H. Wapstrab, and C. Thibaulta, Nucl. Phys. **A729**, 337 (2003).

[44] A. Bodek *et al.*, Phys. Rev. D **20**, 1471 (1979).

[45] W. Melnitchouk, R. Ent, and C. Keppel, Phys. Rep. **406**, 127 (2005).

[46] S. Kumano, Int. J. Mod. Phys. Conf. Ser. **40**, 1660009 (2016); see also contributions to Workshop on Hadron physics with high-momentum hadron beams at J-PARC in 2013 and 2015, http://www-conf.kek.jp/past/hadron1/j-parc-hm-2013/, http://research.kek.jp/group/hadron10/j-parc-hm-2015/.

[47] For information on the ILC project, see http://www.linearcollider.org. On the TESLA-N, see http://tesla.desy.de/new_pages/TDR_CD/start.html.